Computational and Experimental Study of Steady Two-dimensional Axisymmetric Non-premixed Methane Counterflow Flames

Giuliano Amantini[1], Jonathan H. Frank[2], Mitchell D. Smooke[1] and Alessandro Gomez[1]

[1]Department of Mechanical Engineering

Yale Center for Combustion Studies

Yale University, New Haven, CT 06520, USA

alessandro.gomez@yale.edu

[2]Combustion Research Facility

Sandia National Laboratories

Livermore, CA 94551, USA

jhfrank@ca.sandia.gov

A steady two-dimensional axisymmetric methane/enriched-air laminar opposed-jet diffusion flame is investigated computationally and experimentally. The emphasis is on achieving a quantitative agreement between computations and experiments, in order to use the validated computational resources for predictive purposes in a broader range of scenarios, including the flamelet approach to turbulent combustion. This goal has eluded the combustion community to date, although the two-dimensional problem has received some attention both under the steady and the unsteady configurations, mainly for methane and hydrogen flames. Santoro *et al.*, [1-3] analyzed vortex-flame interaction and propagation of edge flames in counterflow mixing layers along the burner axis of symmetry, both computationally and experimentally. Frouzakis *et al.*, [4] simulated two-dimensional hydrogen flames and examined the sensitivity of such flames to the inlet boundary conditions. Lee *et al.*, [5] and Frouzakis *et al.*, [6] have studied the transition from a diffusion to an edge hydrogen flame. Katta *et al.*, [7-9] investigated the interaction between different types of perturbations in hydrogen flames, identifying various quenching patterns. Although some comparisons between experimental and computational results were attempted in the two-dimensional unsteady case [9], they were only qualitative in nature and limited only to OH. The interaction between a single vortex and a methane counterflow flame was simulated in Oh et al. [10].

Here, we measured experimentally the forward reaction rate (RR) of the reaction $CO + OH \rightarrow CO_2 + H$ by simultaneous imaging of single-photon OH LIF and two-photon CO LIF. Further, particle image velocimetry (PIV) was used to measure velocities in the proximity of the fuel and oxidizer nozzles, providing detailed boundary conditions for the computational simulations, and additional experimental data in the cold region of the flame. These techniques were applied and documented in an experimental study on vortex flame interaction in the same configuration [11]. Although quantitative modeling and validation of

the unsteady two-dimensional problem is the ultimate goal, especially in the context of the re-ignition, the steady counterpart, addressed here, is an indispensable first step.

Computationally, the study employs a vorticity-velocity formulation, which has many attractive features. First, pressure does not explicitly appear in the differential equations, and thus difficulties associated with the determination of the pressure boundary conditions, especially at the outflow boundary, are avoided. Second, the boundary conditions for this formulation are easier to impose than those based on streamfunction or vector-potential formulations. Third, vorticity boundary conditions placed at the wall couple the vorticity to the velocity field through the kinematic definition. In the present study, two vorticity-velocity formulations are taken into account, and it is shown that the formulation described in [12] experiences mass losses. In order to obtain a mass-conservative solution, the Poisson-like equation for radial velocity is replaced by the continuity equation, and mass conservative solutions that closely match the experimental data are obtained.

Figure 1 presents computed and experimental results for CO number density for a typical flame. The composition of this flame in mole fraction is 0.209% methane diluted in nitrogen and 0.368% oxygen diluted in nitrogen. Fuel is issued from the top and oxidizer from the bottom nozzle. Since the burner is axisymmetric, only half of the domain is shown. On the leftmost side of the images is the axis of symmetry of the burner, and on the rightmost side is the outlet. The radial length of the images is *3.2 cm* and the axial length is *1.2 cm*. The CO layer thins slightly as we move away from the axis of symmetry, then progressively thickens as we move out of the nozzle region toward the outer boundary. The initial thinning of the layer is explained by the higher transverse velocity in the proximity of the nozzle walls, which is a peculiarity of the counterflow configuration as compared to more uniform velocity profiles obtained for free jets. Outside the nozzle region, both components of the velocity vector decrease and the prevailing strain rate reduction accounts for the progressive thickening of the CO layer. The CO produced in the hot region is entrained by the top recirculation and carried in the cold boundary in the proximity of the nozzle exit. The agreement between the computational and the experimental results for the CO number density layer is remarkable, and it validates the ability of the computation to capture the structure of the CO layer quantitatively. Mild disagreement is observed in the region close to the top water-cooled flange. However, at very low temperatures the proportionality between CO LIF and CO number density breaks down, and in such a region the experimental results are not sufficiently quantitative.

Figure 2 shows the forward reaction rate for the reaction $CO + OH \rightarrow CO_2 + H$. Both the experimental and the numerical results indicate that the flame is extremely flat even in the outermost zone, that is far from the nozzle region. This is possibly due to the fact that the heavier oxidizer stream is issued from the bottom burner and the lighter fuel stream is issued from the top burner. The agreement between the computational and numerical shape of the layer is quantitative both in the nozzle region and in the outermost region. Additional comparisons for the velocity field, capturing the structure of the recirculations anchored at the nozzles exits, will be presented at the Symposium.

We conclude that the goal of developing a two-dimensional model of counterflow flames, anchored by an experimental validation with multiple variables, has been achieved. The model can now be used to assess the importance of some flame observables as tracers of heat release and scalar dissipation. The mixing layer thickness is well represented by those of CO_2, H_2O and N_2 whereas it is poorly correlated with those of OH, of CH_2O, and of the reaction rates $CO + OH \rightarrow CO_2 + H$ and $CH_2O + OH \rightarrow CHO + H_2O$, in contrast with the one-dimensional analysis in [12]. We also confirmed that the stoichiometric scalar

dissipation rate is correlated with the mixing layer thickness according to a power law, with a coefficient that closely matches the phenomenological expression:

$$\delta_m^2/D_T \sim 1/\chi_{st},$$

where δ_m is the thickness of the mixing layer, D_T is the mass diffusivity coefficient and χ_{st}, is the scalar dissipation rate. Additionally, the decay of the stoichiometric scalar dissipation rate was analyzed in the radial direction as the flow moves out of the nozzle region toward the outlet of the burner and was found to be exponential, in contrast with [2].

References

1. Santoro, V.S., Kyritsis, D.C., Gomez, A., Proc. Combust. Inst. 28 (2000) 1023-1030.
2. Santoro, V.S., Linan, A., Smooke, M.D., Gomez, A., Proc. Combust. Inst. 28 (2000) 2039-2046.
3. Santoro, V.S., Kyritsis, D.C., Smooke, M.D., Gomez, A., Proc. Combust. Inst. 29 (2002) 2227-2233.
4. Frouzakis, C.E., Lee, J., Tomboulides, A.G., and Boulouchos, K., Proc. Combust. Inst. 27 (1998) 571-577.
5. Lee, J., Frouzakis, C.E., Boulouchos, K., Proc. Combust. Inst. 28 (2000) 801-806.
6. Frouzakis, C.E., Tomboulides, A.G., Lee, J., and Boulouchos, K., Proc. Combust. Inst. 29 (2002) 1581-1587.
7. Katta, V.R., Carter, C.D., Fiechtner, G.J., Roquermore, W.M., Gord, J.R., Rolon, J.C., Proc. Combust. Inst. 27 (1998) 587-594.
8. Katta, V.R., and Roquermore, W.M., Proc. Combust. Inst. 28 (2000) 2055-2062.
9. Katta, V.R., Meyer, T.R., Brown, M.S., Gord, J.R., Roquermore, W.M., Combust. Flame 137 (2004) 198-221.
10. Oh, C.B., Lee, C.E., Park, J., Combust. Flame 138 (2004) 225-241.
11. Amantini, G., Frank, J.H., Gomez, A., Proc. Combust. Inst. 30 (2004).
12. Bijjula, K., Kyritsis D. C., Proc. Combust. Inst. 30 (2004)
13. Ern, A. PhD thesis (1994)

Figures

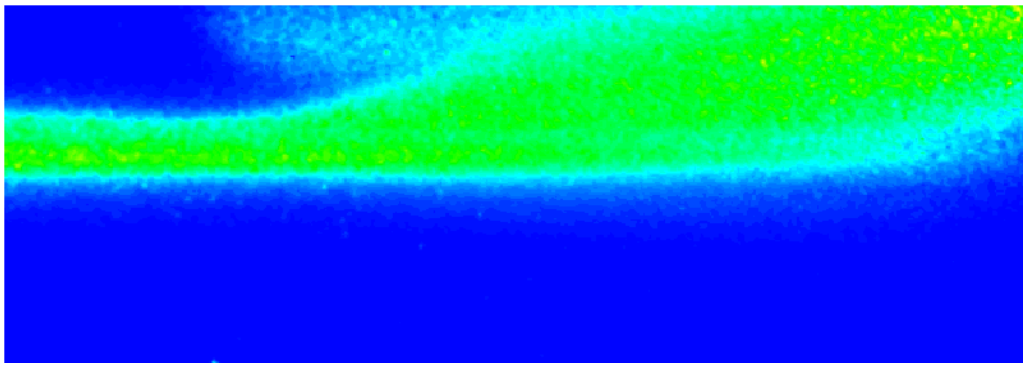

(a)

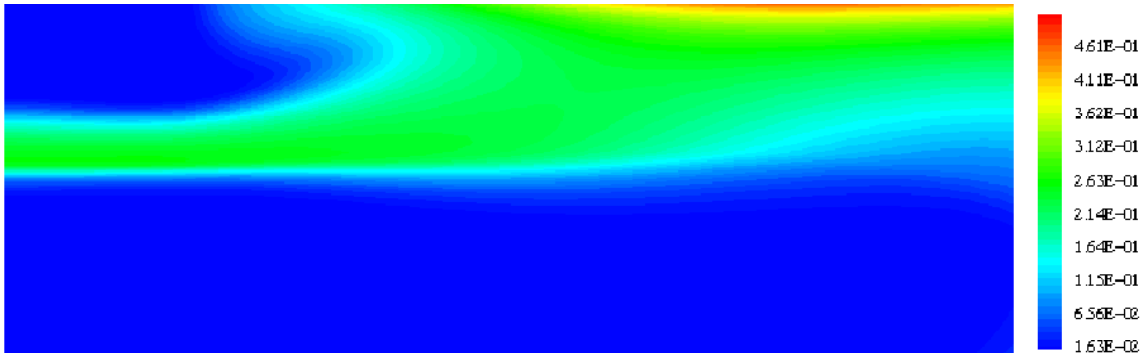

(b)

Figure 1. Experimental (a) and computational (b) CO number density, only half domain is shown. The axis of symmetry of the burner is located at the leftmost side, the outlet is the rightmost side of the images.

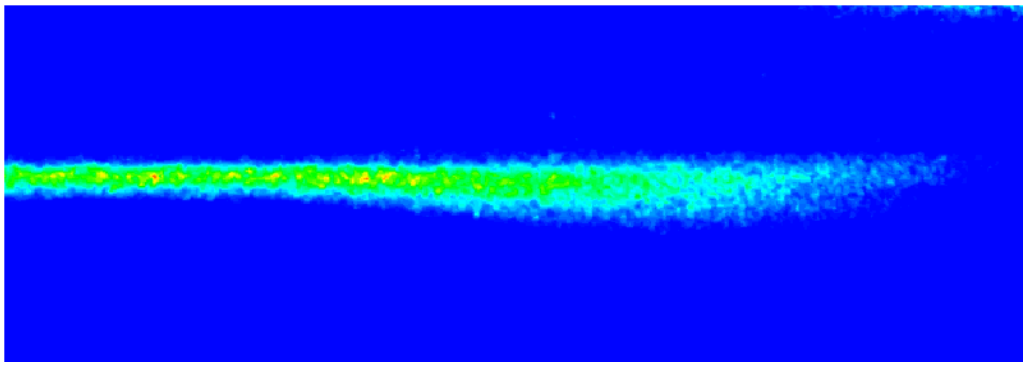

(a)

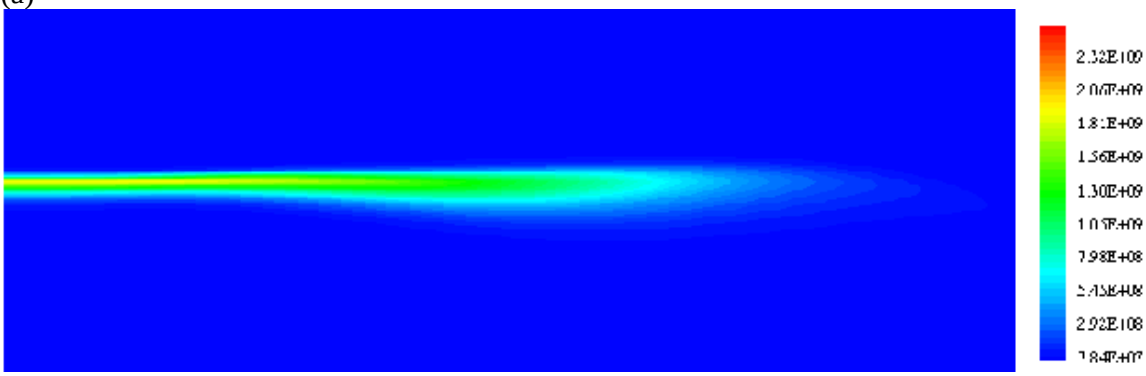

(b)

Figure 2. Experimental (a) and computational (b) reaction rate.